Direct measurement of antiferromagnetic domain fluctuations

O. G. Shpyrko[1], E. D. Isaacs[1,2], J. M. Logan[2], Yejun Feng[2], G. Aeppli[3], R. Jaramillo[2], H. C. Kim[2], T. F. Rosenbaum[2], P. Zschack[4], M. Sprung[4], S. Narayanan[4] and A. R. Sandy[4]

[1]*Center for Nanoscale Materials, Argonne National Laboratory, Argonne, IL 60439, USA*

[2]*James Franck Institute and Dept. of Physics, University of Chicago, Chicago, IL 60637, USA*

[3]*London Centre for Nanotechnology and Department of Physics and Astronomy, University College London, London WC1E 6BT, UK*

[4]*Advanced Photon Source, Argonne National Laboratory, Argonne, IL 60439, USA*

Measurements of magnetic noise emanating from ferromagnets due to domain motion were first carried out nearly 100 years ago [1] and have underpinned much science and technology [2, 3]. Antiferromagnets, which carry no net external magnetic dipole moment, yet have a periodic arrangement of the electron spins extending over macroscopic distances, should also display magnetic noise, but this must be sampled at spatial wavelengths of order several interatomic spacings, rather than the macroscopic scales characteristic of ferromagnets. Here we present the first direct measurement of the fluctuations in the nanometre-scale spin- (charge-) density wave superstructure associated with antiferromagnetism in elemental Chromium. The technique used is X-ray Photon Correlation Spectroscopy, where coherent x-ray diffraction produces a *speckle* pattern that serves as a "fingerprint" of a particular magnetic domain configuration. The temporal evolution of the patterns corresponds to do-

main walls advancing and retreating over micron distances. While the domain wall motion is thermally activated at temperatures above 100K, it is not so at lower temperatures, and indeed has a rate which saturates at a finite value – consistent with quantum fluctuations - on cooling below 40K. Our work is important because it provides an important new measurement tool for antiferromagnetic domain engineering as well as revealing a fundamental new fact about spin dynamics in the simplest antiferromagnet.

Because of scientific and technical interest in ferromagnetic domains, there has been large, long-standing activity on magnetic noise in ferromagnets as a direct witness of domain motion. As antiferromagnets begin to find applications themselves, for example as pinning layers in spintronics, there is a need for measurements of the noise associated with moving antiferromagnetic domains. Antiferromagnetic domain dynamics are also important because they are implicated in basic problems in condensed matter physics, such as high temperature superconductivity and 'heavy' Fermions. Neutrons are an excellent non-local probe of antiferromagnetism and its dynamics [4]. However, a direct *local* probe of mesoscopic antiferromagnetic domain dynamics has not been hitherto available because the magnetic dipole moments for antiferromagnets vanish on the scale of a nanometer, rendering the domain fluctuations responsible for noise essentially invisible to the direct magnetometer probes (e.g. superconducting interference devices) which have been so successful for ferromagnets [5].

Chromium is a body-centred cubic (bcc) metal with an antiferromagnetic state nearly described by the simple rule that the electrons surrounding each Cr atom have magnetization oppo-

site to those on the nearest neighbour Cr atoms. What actually occurs is sinusoidal modulation of this elementary magnetic structure, called a spin density wave (SDW) with wavelength λ=6-8 nm, along one of the three equivalent cubic (100) directions. A single crystal chromium sample cooled below the Néel temperature T_N=311 K spontaneously breaks (see Fig. 1) into three types of magnetic domains characterized by the three different choices for the SDW propagation direction [6]. The SDW is accompanied by a charge density wave (CDW), a combination of both itinerant and ionic charge modulation.

X-ray microdiffraction reveals that the typical size of the SDW domains in bulk Cr samples is on the order of 1-30 μm [7]. Fluctuations of domain walls at fixed temperature have been studied via random electrical telegraph noise in thin Cr films for temperatures above 140 K [8]. Even though the measurements were done for mesoscopic samples, the effects on the electrical resistance R of the switching dynamics were small (δR/R$\sim 10^{-5}$) and the interpretation difficult because R is an indirect probe of the underlying SDW and CDW order.

We report the first direct observations of domain wall fluctuations in bulk Cr using X-ray Photon Correlation Spectroscopy (XPCS), which overcomes the limitations of the classic bulk and laser probes in that it accesses the short wavelength structure associated with the SDW directly. A coherent beam illuminating a partially ordered system (in our case consisting of SDW/CDW domains) produces an interference pattern, also known as *speckle* [9, 10]. Due to the high sensitivity of speckle to minute changes in domain wall configuration, the time variation of the speckle pattern directly reveals the dynamics of domain structure. Fig. 2a is a schematic of the experi-

mental configuration, and Figure 2b shows a speckle pattern of the (200) Bragg peak for the bcc Cr lattice. Interference fringes arising from partial coherence of the x-ray beam are clearly seen in the image as well as in the line scans shown in Fig. 2c. Incoherent diffraction would produce the Gaussian-like profile represented by the black line in Fig. 2c. The lattice Bragg speckle pattern is static over 5 hrs indicating the high level of stability for our instrumentation and the sample.

We turn next to the speckle pattern for the (2-2δ, 0, 0) CDW superlattice reflection, displayed for 17 K at a variety of times in Fig. 3b. The patterns in subsequent frames, separated by 1,000 s, grow increasingly dissimilar for longer time lags – patterns within frames collected more than 3,000 s apart appear completely uncorrelated. Thus, the CDW speckle evolves with a characteristic time of a few thousand seconds or less, much shorter than the $>$20,000 s relaxation time for the bcc Bragg speckle of Fig. 2c. This indicates that the changes in the CDW speckle are indeed due to changes in the magnetic domain configuration, rather than some experimental artefact. For example, drift of the x-ray beam or the cryostat, motion of crystalline defects within the Cr sample or any other effect not related to magnetic domain dynamics would inevitably cause changes in *both* the CDW and (200) Bragg speckle.

The spatial sensitivity of the speckle to domain motion is described by two distinct lengths: the first is $1/\Delta Q \sim 100$Å, where $\Delta Q = 10^{-2}$Å^{-1} is the total size of visible speckle pattern in reciprocal space (See Figs. 2b, 2c and 3b) and represents the minimum size of domains with a visible impact on the speckle pattern. The second is the domain wall displacement necessary to produce a speckle pattern that is highly dissimilar (or uncorrelated) to the original one. A combination of

x-ray microdiffraction images of domain configurations and speckle simulations indicate that this second length is 1 μm (see Methods and Supplementary Information).

Beyond revealing that domain walls are moving by distances of order 1 μm, the data provide several other important quantities. For example, we can evaluate the autocorrelation function $g_2(t)$:

$$g_2(t) = \frac{\langle I(\tau)I(\tau+t)\rangle_\tau}{\langle I(\tau)\rangle_\tau^2} = 1 + A\,|F(Q,t)|^2 \quad (1)$$

where I(τ) and I($\tau+t$) are the intensities in a given pixel for frames taken at times τ and τ+t respectively, F(Q,t) is the intermediate scattering function, A describes the beam coherence [9,10], and the averaging is performed over times τ and pixels. Figure 3a shows $|F(Q,t)|^2$for several temperatures calculated from the CDW speckle. For large time delays the speckle patterns become uncorrelated, resulting in $g_2(t)=1$, corresponding to $|F(Q,t)|^2 =0$. The dynamics are strongly temperature-dependent: upon cooling, the domain fluctuation times increases by nearly two decades. Surprisingly, below 40 K the times remain finite, rather than diverging as expected for thermally driven fluctuations.

Two distinct fluctuation timescales are visible in most datasets presented in Fig. 3a. The measured |F(Q,t)| was therefore modelled by a double exponential form:

$$|F(Q,t)| = a\exp[-(t/\tau_F)^\beta] + (1-a)\exp[-(t/\tau_S)^\beta] \quad (2)$$

A small value of a=0.03-0.10 indicates that the time dependence of |F(Q,t)| is mainly due to slow fluctuations. The value of the stretching exponent β was found to be greater than 1, manifested by the "compressed" shape of the |F(Q,t)|. Compressed exponential relaxation has been observed

for a variety of soft matter systems undergoing "jamming" transitions which results in arrested, solid-like collective dynamics [11, 12, 13] with β >1, as instead of liquid-like fluctuations with $\beta \leq$1. Extended to our system, this points to elastically coupled dynamics between blocks of spins, similar to elastic collective depinning dynamics observed in CDW conductors [14], an observation also consistent with the weakly pinned nature of SDW/CDW domains [15-17]. Furthermore, the fit value of β at T<100K is approximately 1.5 (Fig. 4b), a universal value for dynamics of soft condensed matter systems in a jammed state [18].

Fig. 4 shows the T-dependence of the slow relaxation times τ_S obtained from fits to autocorrelation functions in Fig. 3a. The 20% uncertainty in fitting parameters $\tau_S$arises primarily from counting statistics of the autocorrelation function $g_2(t)$ (see Supplementary Information). Standard thermal activation ($\tau_t^{-1} = f_o \exp(-\Delta E/k_B T)$, blue line) with a single attempt frequency f_o and activation barrier $\Delta E/k_B = 240 \pm 50K$ accounts for the data at high T. The thermal picture fails spectacularly at low temperature for T<40 K, and a switching mechanism which is temperature-independent in this range is required. The simplest possibility is that switching between low-energy domain wall configurations occurs via quantum tunneling, rather than classical thermal activation. A fit to the data that combines a thermally activated model and a quantum tunneling contribution represented by a temperature-independent residence time τ_{QT}, $\tau_S^{-1} = \tau_{QT}^{-1} + \tau_R^{-1} \exp(-\Delta E/k_B T)$ is shown by the red solid line in Fig. 4 for τ_{QT}=5,000 s and τ_R =15 s (confidence limits obtained from the fits are τ_{QT}=5,000$\pm$1,000 s and t_R=4-60 s). The short-term fluctuation rate τ_F^{-1} observed in the autocorrelation data in Fig. 3a has the same magnitude as the attempt frequency τ_R^{-1}. In analogy with alpha and beta relaxation observed in glasses, supercooled liquids and jammed soft

matter systems, faster fluctuations represent local relaxation, while slower fluctuations are due to collective relaxation modes.

The relaxation times observed here are similar to those associated with magnetization switching in ferromagnets first observed by Barkhausen [1] and studied since then in systems from bulk materials to magnetic molecules [5, 19-22]. Antiferromagnets have more complex order than ferromagnets because they break translation as well as spin rotation invariance, which has forced us to formulate a very crude physical picture, to understand our data at a semi quantitative level. We start with the realization that to minimize the very large exchange energy ($>$0.4 eV) [23, 24] associated with domain walls, it is clearly advantageous for the nodal planes (where the spin polarization vanishes) of the SDW with its propagation vector perpendicular to the domain wall to lie on the walls [25]. Such an assumption is further supported by the previously observed preference for the formation of SDW nodes at Fe/Cr interfaces [26]. This implies that the fundamental switching unit (grey shaded region in Fig. 1a) is of volume $V_S \sim (\lambda/2)^3$ where λ is the underlying period of the SDW. In the simplest Gaussian model where underlying units are switching randomly at typical times τ_U, we would conclude that the switching time for a volume of V=1 μm^3 would be (V/V$_S$)$^2\tau_U$. Using our experimental value for the attempt frequency τ_R^{-1}, we therefore obtain τ_U^{-1}= 36 THz=140 meV as the attempt frequency for rotating an entire unit. This is an electronic energy scale, and could therefore be derived from the hopping of electrons across the domain wall; such electrons (also important in electrical noise measurements [8]) are, after all, responsible for the current fluctuations which sample the possibility of rotating the Fermi surface of a 'quantum dot' with the fundamental unit volume V$_S$. It is fortunate that the barrier for rotation between

two minima has been identified by neutron spectroscopy on $Cr_{0.95}V_{0.05}$ (data for pure Cr are not published) (See Fig. 2 of Ref. 27) as the energy E_o at which the incommensurate spin density fluctuations no longer display distinct peaks at the incommensurate satellite positions; E_o is found to be of order 25 meV (or 290 K), which is not far from the tunnelling barrier ΔE=20 meV (or 240 K) established in our own experiments. Interestingly, it is this energy, rather than the much larger exchange coupling, which corresponds to T_N.

In the simplest WKB approximation (see e.g. Ref. 22), the dimensionless ratio $\tau_R/\tau_{QT}$is equal to $\exp(-S/\hbar)$, where $S = \sqrt{I\Delta E}$ is the tunneling action. Because the underlying attempt frequencies and their rescaling to account for observable effects in the X-ray experiment are the same for both incoherent quantum and classical processes, all of the detail – invoking multiple rotors - of the last paragraph drops out, and S characterizes a single rotor. We can therefore calculate the moment of inertia I of the quantum rotor using the measured parameters τ_{QT}, τ_R and the barrier height ΔE=20 meV obtained from the Arrhenius regime. The result is I=100 m_e nm^2, which, assuming a cube of uniform density distributed over the $(\lambda/2)^3$ volume of the fundamental unit corresponds to 0.1 electron mass m_e per Chromium unit cell. This remarkable result, derived only from our data and the simple physical picture of Fig. 1, is consistent with Hall effect data [28, 29] showing that the SDW is associated with the loss of a similar number of carriers, which of course must be moved with the rotors when there is a switching event.

We have introduced the direct measurement of noise spectra in *antiferromagnets*. Our experiments access local mesoscale spin dynamics with just a few domain walls in the illuminated

volume, an advantage over non-local experimental probes that cannot be easily applied for macroscopic or bulk structures. The key finding is that even in bulk samples, and at temperatures very low compared to the Neel temperature, domain walls can be unstable on time scales of fractions of an hour. What this means is that the stability of antiferromagnetism needs to engineered, e.g. by insertion of appropriate pinning centres, into devices that exploit it. This will become even more important for nanoscale spintronics including antiferromagnetic elements. Beyond the obvious advantages for magnetic engineering of now having a technique with which antiferromagnetic domain fluctuations can be readily assessed, we foresee tremendous opportunities in areas such as the science of antiferromagnetic nanoparticles.

Methods. Experiments were carried out at beamlines 33-ID and 8-ID of Advanced Photon Source, Argonne National Laboratory. The undulator-generated x rays are monochromatized by a Si (111) crystal at an energy E=7.35 keV (wavelength 1.686 Angstroms). A 10 μm pinhole aperture or a 10gμm (horizontally) by 40 μm (vertically) slits placed 5 cm upstream from the sample selected partially coherent portion of the x-ray beam with a resulting coherence fraction A$\approx$0.07-0.18. A high purity (111) Cr wafer (Alfa Aesar, Ward Hill, MA) was used to ensure roughly equal population of domains. The sample was mounted inside a low-drift He flow cryostat, with thermal shielding provided by 600 μm thick Be dome. Speckle patterns were recorded with a Princeton Instruments PI-LCX 1300 deep depletion x-ray CCD camera (1340x1300 pixel array with 20 micron by 20 micron pixel size), located 150 cm from the sample in reflection geometry.

References.

[1] Barkhausen, H. Zwei mit Hilfe der Neuen Verstärker entdeckte Erscheinungen. *Phys. Z.* **20**, 401-403 (1919).

[2] Weissman, M. B. Low Frequency Noise as a tool to study disordered materials. *Annu. Rev. Mater. Sci.* **26**, 395-429 (1996).

[3] Sethna, J. P., Dahmen, K. A. & Myers C. R. Crackling Noise. *Nature* **410**, 242-250 (2001).

[4] Ekspong, G. (ed.) *Nobel Lectures, Physics 1991-1995* (World Scientific Publishing Co., Singapore, 1997). 1994 Nobel prize lectures by Clifford G. Shull and Bertram N. Brockhouse (pp. 107-154)

[5] Vitale, S., Cavalieri, A., Cerdonio, M., Maraner, A. & Prodi, G. A. Thermal equilibrium noise with 1/f spectrum in a ferromagnetic alloy: Anomalous temperature dependence. *J. Appl. Phys.* **76**, 6332-4 (1994).

[6] For a review of SDW in Cr see Fawcett, E. Spin-density-wave antiferromagnetism in chromium. *Rev. Mod. Phys.* **60**, 209-283 (1988).

[7] Evans, P.G., Isaacs, E.D., Aeppli, G., Cai, Z.-H. & Lai, B. X-ray microdiffraction image of antiferromagnetic domain evolution in chromium. *Science* **295**, 1042-1045 (2002).

[8] Michel, R. P., Israeloff, N. E., Weissman, M. B., Dura, J. A. & Flynn, C. P. Electrical-noise measurements on chromium films. *Phys. Rev. B* **44**, 7413-7425 (1991).

[9] Sutton, M., Mochrie, S. G. J., Greytak, T., Nagler, S. E. & Berman, L. E. Observation of speckle by diffraction with coherent X-rays. *Nature* **352**, 608-610 (1991).

[10] Sutton, M. Coherent X-ray Diffraction. In Mills, D. (ed.) *Third-Generation Hard X-Ray Synchrotron Radiation Sources: Source Properties, Optics, and Experimental Techniques* (John Wiley

& Sons, New York, 2002).

[11] Cipelletti, L., Manley, S., Ball, R. C. & Weitz, D. A. Universal Aging Features in the Restructuring of Fractal Colloidal Gels. *Phys. Rev. Lett.* **84**, 2275–2278 (2000).

[12] Bandyopadhyay, R. *et al.* Evolution of Particle-Scale Dynamics in an Aging Clay Suspension. *Phys. Rev. Lett.* **93**, 228302 (2004).

[13] Falus, P., Borthwick, M. A., Narayanan, S., Sandy, A. R. & Mochrie, S. G. J. Crossover from Stretched to Compressed Exponential Relaxations in a Polymer-Based Sponge Phase. *Phys. Rev. Lett.* **97**, 066102 (2006).

[14] Lemay, S. G., Thorne, R. E., Li Y. & Brock, J. D. Temporally ordered collective creep and dynamic transition in the charge-density-wave conductor NbSe3. *Phys. Rev. Lett.* **83**, 2793-2796 (1999).

[15] Fukuyama H.& Lee, P. A. Dynamics of the charge-density wave. I. Impurity pinning in a single chain. *Phys. Rev. B* **17**, 535 - 541 (1978).

[16] Fukuyama H.& Lee, P. A. Dynamics of the charge-density wave. II. Long-range Coulomb effects in an array of chains. *Phys. Rev. B* **17**, 542 - 548 (1978).

[17] Littlewood, P. B. & Rice, T. M. Metastability of the Q Vector of Pinned Charge- and Spin-Density Waves. *Phys. Rev. Lett.***48**, 44 - 47 (1982).

[18] Cipelletti, L. *et al.* Universal non-diffusive slow dynamics in aging soft matter. *Faraday Discuss.* **123**, 237-251 (2003).

[19] Chudnovsky, E. M. & Tejada, J. *Macroscopic Quantum Tunneling of the Magnetic Moment* (Cambridge University Press, Cambridge, UK, 1998).

[20] Barbara, B. *et al.* Quantum tunneling in magnetic systems of various sizes. *J. Appl. Phys.* **73**, 6703-6706 (1993).

[21] Wernsdorfer, W. Classical and quantum magnetization reversal studied in nanometersized particles and clusters. *Adv. Chem. Phys.* **118**, 99 (2001).

[22] Brooke, J., Rosenbaum, T. F. & Aeppli, G. Tunable quantum tunnelling of magnetic domain walls. *Nature*, **413**, 610-613 (2001).

[23] Fenton, E. W. & Leavens, C. R. The spin density wave in chromium. *J. Phys. F* **10**, 1853-1878 (1980).

[24] Fenton, E. W. Domains in the Spin-Density-Wave Phases of Chromium. *Phys. Rev. Lett.* **45**, 736 - 739 (1980).

[25] Michel, R. P., Weissman, M. B., Ritley, K., Huang, J. C. & Flynn, C. P. Suppression of polarization fluctuations in chromium alloys with commensurate spin-density waves. *Phys. Rev. B* **47**, 3442 - 3445 (1993).

[26] Fullerton, E. E., Bader, S. D. & Robertson, J. L., Spin-density-wave Antiferro-magnetism of Cr in Fe/Cr(001) Superlattices, *Phys. Rev. Lett.* **77**, 1382-1385 (1996).

[27] Hayden, S. M., Doubble, R., Aeppli, G., Perring, T. G. & Fawcett, E. Strongly Enhanced Magnetic Excitations Near the Quantum Critical Point of $Cr_{1-x}V_x$ and Why Strong Exchange Enhancement Need Not Imply Heavy Fermion Behavior. *Phys. Rev. Lett.* **84**, 999 - 1002 (2000).

[28] Lee, M., Husmann, A., Rosenbaum, T. F. & Aeppli, G. High resolution study of magnetic ordering at absolute zero. *Phys. Rev. Lett.* **92**, 187201 (2004).

[29] Yeh, A. *et al.* Quantum phase transition in a common metal. *Nature* **419**, 459-462 (2002).

Supplementary Information accompanies the paper.

Acknowledgements Use of the Center for Nanoscale Materials and Advanced Photon Source was supported by the U. S. Department of Energy, Office of Science, Office of Basic Energy Sciences. The work at the University of Chicago was supported by the National Science Foundation, while that in London was funded by a Royal Society Wolfson Research Merit Award and the Basic Technologies programme of RCUK. Authors declare they have no competing financial interests.

Competing Interests The authors declare that they have no competing financial interests.

Correspondence Correspondence and requests for materials should be addressed to O. G. S. (oshpyrko@anl.gov)

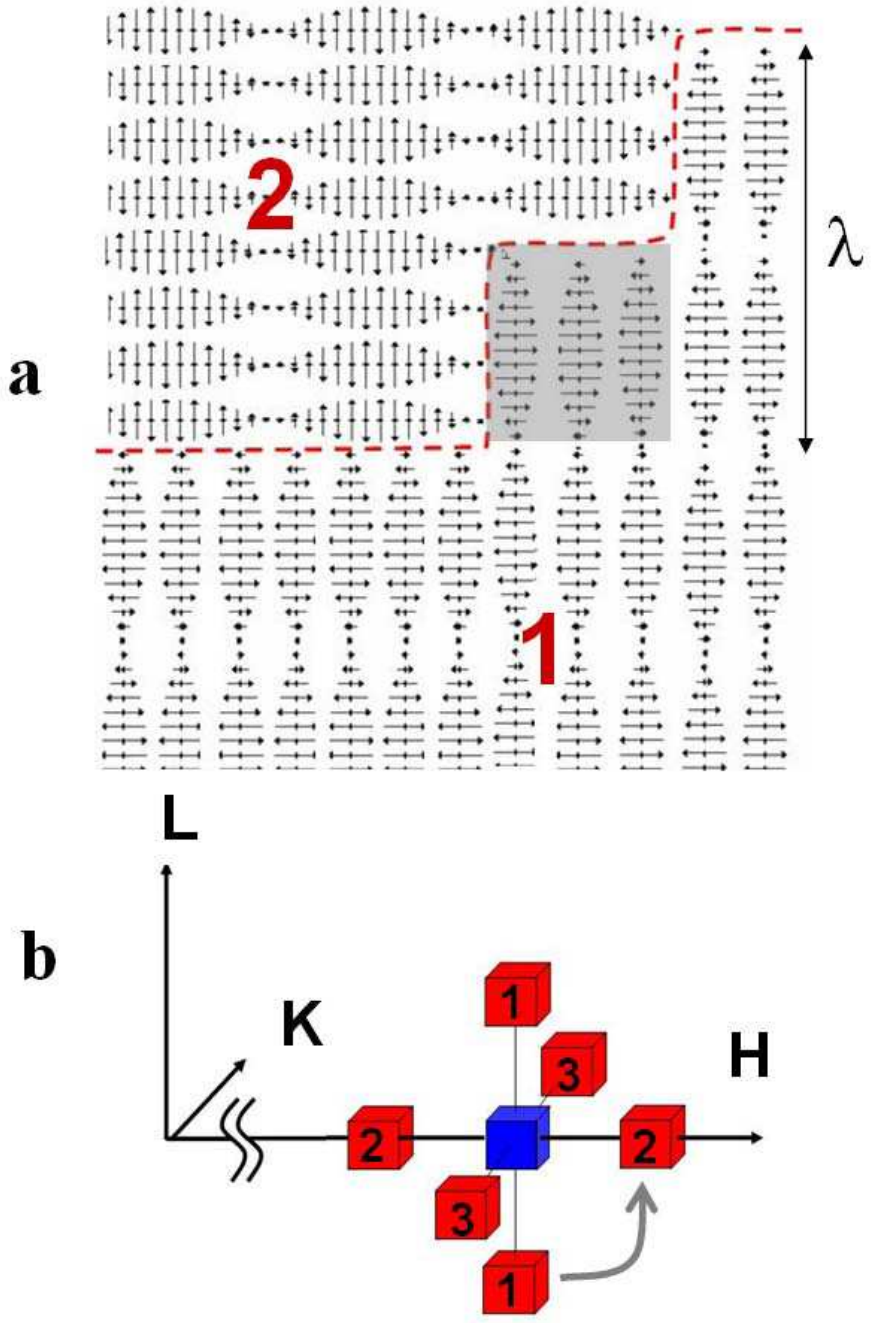
a
2
1
λ
b
L
K
H
1
3
2
2
3
1

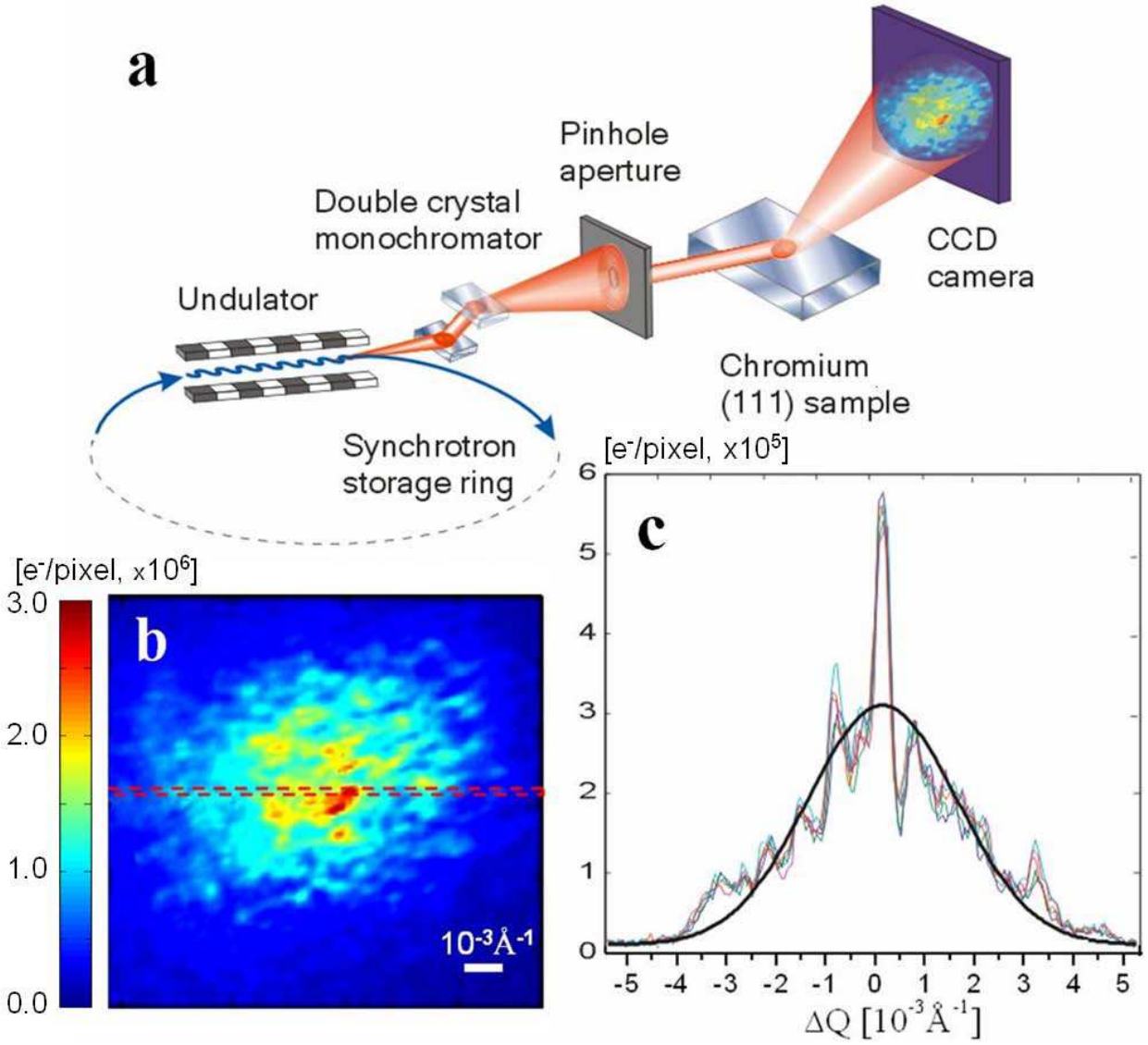
a
Pinhole
aperture
Double crystal
monochromator
CCD
camera
Undulator
Chromium
(111) sample
Synchrotron
storage ring
[e⁻/pixel, x10⁶]
3.0
2.0
1.0
0.0
b
10⁻³Å⁻¹
[e⁻/pixel, x10⁵]
c
6
5
4
3
2
1
0
-5 -4 -3 -2 -1 0 1 2 3 4 5
ΔQ [10⁻³ Å⁻¹]

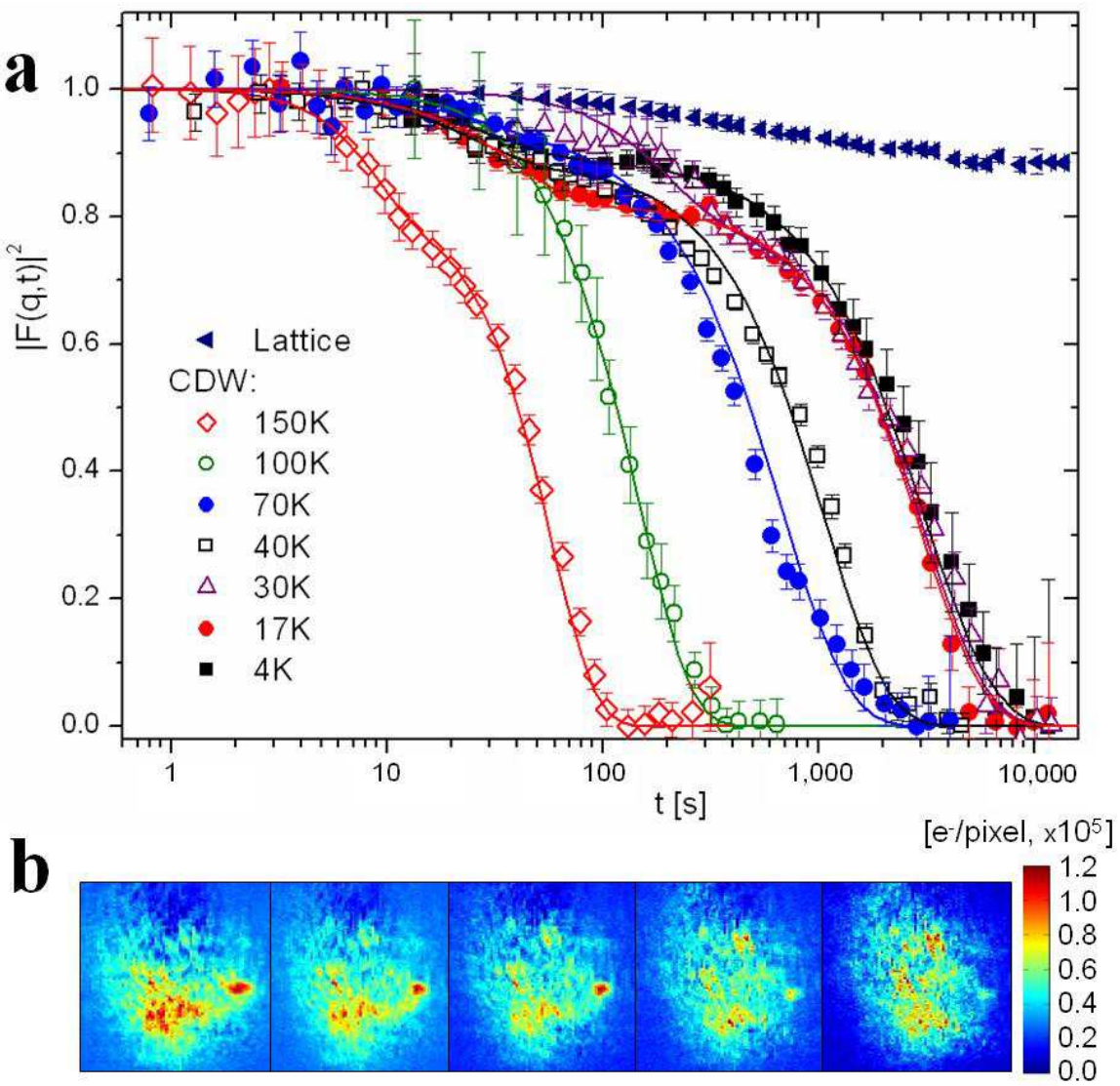
a
1.0
0.8
0.6
0.4
0.2
0.0
|F(q,t)|²
Lattice
CDW:
150K
100K
70K
40K
30K
17K
4K
1
10
100
1,000
10,000
t [s]
b
[e⁻/pixel, x10⁵]
1.2
1.0
0.8
0.6
0.4
0.2
0.0

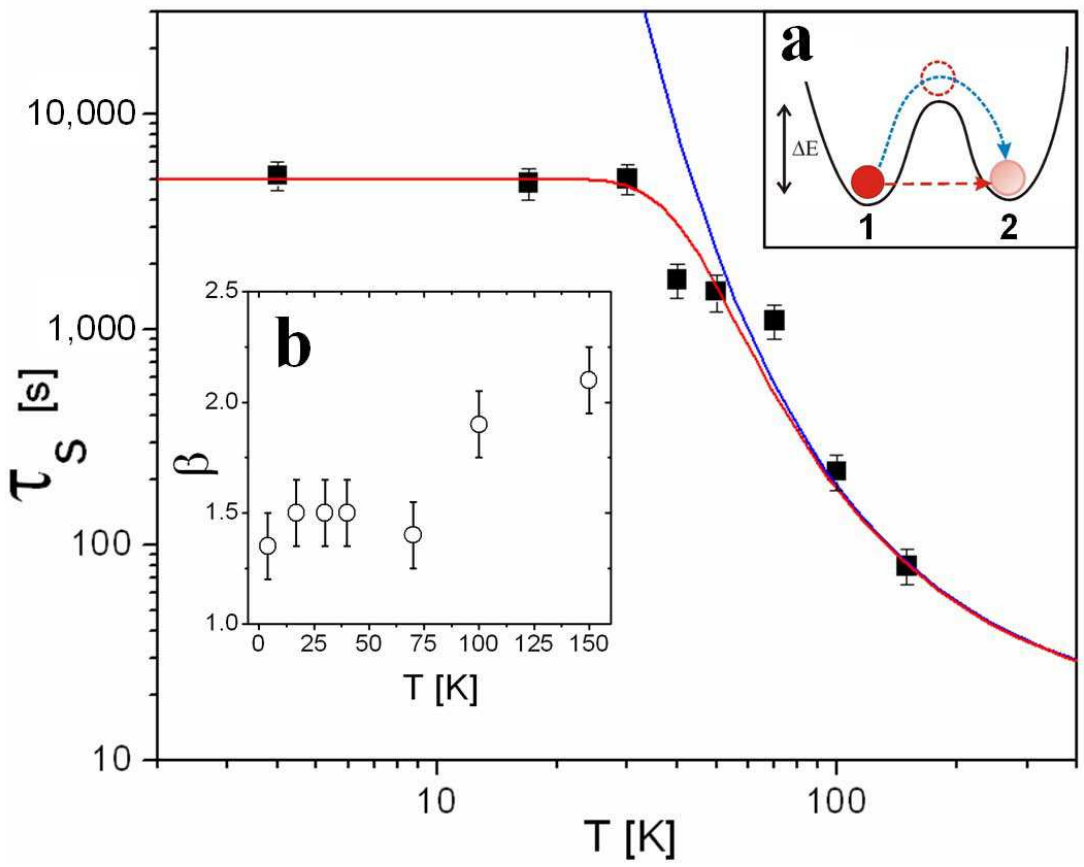
a
ΔE
1
2
b
β
T [K]
τ_S [s]
10,000
1,000
100
10
10
100
T [K]

Figure 1 | **Spin Density Wave Domain Wall in Chromium.** **a**, Schematic representation of the domain wall (red dashed line) separating two regions with perpendicular orientations of transverse spin density wave. The domain wall is shown to propagate along the weak nodal planes – where local magnetization approaches zero. Shaded region represents an elementary domain unit with volume $(\lambda/2)^3$ that can be thought of as a magnetic quantum dot in a cubic lattice of a similar quantum dots. **b**, Reciprocal space configuration of lattice (200) Bragg peak (blue) and six surrounding charge density wave satellites (red). Domains marked as 1 and 2 in **a** contribute to pairs of satellites marked 1 and 2 in **b**, respectively. 90 degree rotation of SDW propagation vector within the shaded elementary volume of domain 1 would realign spins with domain 2, resulting in shift of domain wall and transfer of scattering intensity from satellite pairs 1 to 2, marked with an arrow in **b**.

Figure 2 | **X-ray speckle measurements.** **a**, Schematic of the experimental setup. **b**, CCD image of the x-ray speckle observed for the [200] lattice Bragg reflection. **c**, Intensity distribution for a line scan across a region shown with a bar in (B) panel. Five differently coloured and nearly identical lines represent line scans of the portion of speckle pattern shown with red dashed line in **b**, taken one hour apart. Black line is a simulated statistically averaged Gaussian profile, expected for completely incoherent beam.

Figure 3 | **Autocorrelation of speckle images.** **a,** Intensity autocorrelation data for

[200] lattice Bragg peak as well as for CDW superlattice [2-2δ, 0, 0] peak at T=150 K, 100 K, 70 K, 40 K, 30 K, 17 K and 4 K. Two distinct timescales are clearly present in the CDW autocorrelation function. Solid lines represent theoretical fits to the data. See text for further details. **b,** Time sequence of CDW speckle pattern evolution at 17 K. Subsequent images are taken 1,000 s apart, each image is 10^{-2} Å^{-1}by10^{-2} Å^{-1}.

Figure 4 | **Temperature-dependent domain wall dynamics.**Characteristic slow fluctuation timescale τ_s obtained from fits to autocorrelation function data shown in Fig. 3a, compared to classical Arrhenius model (blue line) and a model that also includes a temperature-independent switching rate term (red line). **a**, Potential energy surface including thermally activated (blue dashed line) and quantum tunnelling (red dashed line) mechanisms of the transition between the two low energy domain configurations 1 and 2 (see Fig. 1 for an example involving elementary switching volume) separated by energy barrier ΔE **b**, Values of stretching exponent β for various temperatures.